ELSEVIER

Journal of Organometallic Chemistry 565 (1998) 141–151

Journal of Organometallic Chemistry

Linking of benzyne and carbon monoxide at a triruthenium centre by migratory insertion[1]

Jonathan P.H. Charmant, Helen A.A. Dickson, Nigel J. Grist, Selby A.R. Knox *, A. Guy Orpen, Kathryn Saynor, Josep M. Viñas

School of Chemistry, University of Bristol, Bristol BS8 1TS, UK

Received 27 November 1997

Abstract

The μ_3-benzyne complex $[Ru_3(CO)_7(\mu\text{-}PPh_2)_2(\mu_3\text{-}C_6H_4)]$ (**1a**) reacts at room temperature (r.t.) with carbon monoxide (1 atm), trimethylphosphite, or *t*-butylisocyanide to give complexes $[Ru_3(CO)_6L_2(\mu\text{-}PPh_2)_2(\mu_3\text{-}C_6H_4CO)]$ (**2a**, L = CO; **2b**, L = $P(OMe)_3$; **2c**, L = ^{t}BuNC) containing an *ortho*-metallated μ_3-benzoyl ligand. Studies with ^{13}CO confirm that the reaction involves a migratory insertion of CO into a benzyne-CO σ-bond. The μ_3-benzoyl products are formed exclusively when a large excess of the π-acceptor ligand is used, but at lower concentrations substitution of CO by the incoming ligand also occurs to give the complexes $[Ru_3(CO)_6L(\mu\text{-}PPh_2)_2(\mu_3\text{-}C_6H_4)]$ [**1b**, L = $P(OMe)_3$; **1c**, L = ^{t}BuNC]. Although ^{13}C-labelling studies show that the reaction of **1a** with CO is irreversible at r.t., it is readily reversed by warming complex **2a** in hexane. No reaction occurs at r.t. between complex **1a** and triphenylphosphine or tri-isopropylphosphine, but on heating in toluene the phosphine-substituted complexes $[Ru_3(CO)_6(PR_3)(\mu\text{-}PPh_2)_2(\mu_3\text{-}C_6H_4)]$ (**1d**, R = Ph; **1e**, R = ^{i}Pr) are formed, which upon carbonylation give complexes $[Ru_3(CO)_7(PR_3)(\mu\text{-}PPh_2)_2(\mu_3\text{-}C_6H_4CO)]$ (**2d**, R = Ph; **2e**, R = ^{i}Pr). The structure of the complexes **2** has been established by an X-ray diffraction study on the tri-isopropylphosphine-substituted cluster **2e**. Benzaldehyde is obtained from complex **2a** by bubbling hydrogen through a heated solution of the complex. A mechanism for the carbonylation of μ_3-benzyne is proposed and implications for metal surface chemistry discussed.

Keywords: Benzyne complex; Tri-isopropylphosphine; X-ray diffraction

1. Introduction

Benzene is known to undergo dissociative chemisorption, i.e. C–H bond cleavage, on transition metal surfaces and likely surface species include phenyl and benzyne [1]. The discovery [2] in this laboratory of a range of polynuclear ruthenium complexes containing benzyne bound to three, four and five metal atoms, therefore provided an opportunity, based on the cluster-surface analogy [3], to gain an insight into the dissociative chemisorption of benzene through an exploration of their reactivity. In this paper the reactions of a triruthenium μ_3-benzyne complex $[Ru_3(CO)_7(\mu\text{-}PPh_2)_2(\mu_3\text{-}C_6H_4)]$ (**1a**) with CO and other π-acceptor ligands are described. These studies reveal that CO undergoes migratory insertion into a benzyne-CO σ-bond, affording an *ortho*-metallated benzoyl ligand which can be removed from the metal centre as benzaldehyde through reaction with dihydrogen, providing a model pathway for a metal surface process. There is also relevance to homogeneous catalysis, in that formation of acyl groups by migratory insertion of carbon monoxide into transition metal–alkyl bonds is a key step in several commercially important processes, e.g. hydroformylation and the Monsanto acetic acid synthesis. The insertion of CO into other types of transition metal–carbon bond has also attracted interest, includ-

* Corresponding author.

[1] Dedicated to Professor Michael Bruce on the occasion of his 60th birthday.

0022-328X/98/$19.00
PII S0022-328X(98)00448-3

Table 1
Analytical, physical and IR data for new complexes

Complex	Colour	M. Wt.[a,b]		Analysis/%[a,c]				ν_{CO} /cm^{-1}[d]				
				C		H						
1b	Red	1043	(1044)	44.96	(44.69)	3.19	(3.35)	2020 m	1996 vs	1953 m		
1c	Red	1000	(1003)	e	(49.20)	e	(3.32)	2159 w[f] 1960 m	2027 w 1941 w	2018 mw	1997 vs	1991 s
1d	Red	1180	(1182)	55.28	(54.96)	3.41	(3.33)	2052 vw 1961 mw	2027 mw 1953 w	2004 vs 1928 vw	1985 w	1972 mw
1e	Red	1075	(1080)	49.88	(50.14)	4.49	(4.21)	2049 vw 1980 m	2026 m 1971 ms	2016 mw 1955 ms	2005 vs 1941 vw	1995 ms 1917 w
2a	Yellow	e	(1004)	47.02	(46.76)	2.93	(2.41)	2085 s 1996 mw	2069 s 1989 m	2026 s 1935 w	2020 m	2012 mw
2b	Yellow	1194	(1196)	43.26	(43.35)	3.55	(3.75)	2037 vs	2020s	2000 m	1968 m	1950 mw
2c	Yellow	g	(1114)	50.77	(52.09)	3.81	(4.55)	2165 m[f]	2027 vs	2014 vs	1962 s	1913 w
2d	Yellow	1238	(1238)	52.98	(52.60)	5.11	(5.50)	2073 vs 1984 w	2030 m 1967 vw	2023 ms 1953w	2003 w	1983 m
2e	Yellow	e	(1136)	49.76	(49.78)	3.94	(4.00)	2073 s 1984w	1946 w 1946w	2058 vw	2023 vs	2001 w

[a] Calculated values in parentheses.
[b] FAB mass spectrometry.
[c] Samples crystallised from dichloromethane-hexane unless otherwise stated.
[d] Hexane solution.
[e] Satisfactory values not obtained.
[f] ν(CN).
[g] Found [M-^{t}Bu]$^+$, $m/z = 1056$.

ing insertion into transition metal–alkyne σ-bonds in metal cluster complexes [4]. A preliminary account of this work has appeared [5].

2. Results and discussion

2.1. Reaction of $[Ru_3(CO)_7(\mu\text{-}PPh_2)_2(\mu_3\text{-}C_6H_4)]$ (1a) with CO

Reaction of the μ_3-benzyne complex **1a** with CO occurs readily and cleanly under mild conditions, with uptake of two molecules of CO. Thus, when CO is bubbled through a dichloromethane solution at r.t., the colour gradually changes from red to yellow over 3 days and IR monitoring reveals a smooth transformation into a single new species. Chromatography then gives yellow $[Ru_3(CO)_8(\mu\text{-}PPh_2)_2(\mu_3\text{-}C_6H_4CO)]$ (**2a**) in near quantitative yield. The reaction is more rapid in toluene under 3 atm of CO, when after 18h a yield of 75% is obtained. Crystals of **2a** proved unsuitable for X-ray diffraction but the structure of the new complex was firmly established by a crystallographic study on a phosphine derivative, as described later. Analytical, IR and mass spectroscopic data for this and other new complexes are given in Table 1 ^{1}H- and ^{31}P-NMR data in Table 2, and ^{13}C-NMR data in Table 3.

The IR spectrum of **2a** shows eight terminal carbonyl stretching bands, reflecting the asymmetry of the complex, but no band could be detected for the benzoyl carbonyl, which presumably absorbs below 1500 cm^{-1}. The 24 benzoyl and phenyl protons present in the molecule are seen as a complicated series of signals in the ^{1}H-NMR spectrum, the broad range of chemical shift values (the signals range from d 7.7 to 6.0) being attributable to aromatic ring current effects in a molecule which contains a crowded arrangement of phenyl and benzoyl rings. Such effects have been confirmed by a ^{1}H–^{1}H COSY-NMR experiment carried out on $[Ru_3(CO)_6\{P(OMe)_3\}_2(\mu\text{-}PPh_2)_2(\mu_3\text{-}C_6H_4CO)]$ (**2b**) (see below). The presence of two inequivalent μ-phosphido ligands is clealry shown by the ^{31}P-NMR spectrum which comprises two doublets, at δ 170.8 and 150.0. The benzoyl carbonyl gives a signal at δ 278.6 in the ^{13}C-NMR spectrum which, like most of the other metal bound carbon nuclei, is split into a doublet of doublets by the two inequivalent phosphorus nuclei. Two signals appear at δ 164.7 and 156.7 due to the carbon nuclei at the substituted positions of the benzoyl ring. These signals are shifted towards the olefinic region of the spectrum, indicating that some localisation of electron density occurs in the ring due to the interaction of these carbon atoms with the metal atom and carbonyl group. Four doublets with large coupling constants are observed for the *ipso*-carbon nuclei of the phenyl rings in the phosphido ligands. These data, in conjunction with the other spectroscopic data for **2a** (Tables 1–3), are consistent with the structure shown in Scheme 1 in which two molecules of CO have been incorporated into **1a** to yield a a novel *ortho*-metallated benzoyl complex.

Table 2
^{1}H- and ^{31}P-NMR data for new complexes

Complex	^{1}H-NMR (δ)[a,b]	^{31}P{^{1}H}-NMR (δ)[a,b]
1b	7.79–6.44 (m, 24H, 4Ph and C_6H_4), 3.49 (d, *J* 12, 9H, $P[OCH_3]_3$)	277.4 (d, *J* 175, PPh_2), 196.0 (dd, *J* 175, 25, PPh_2), 151.2 (d, *J* 25, $P[OCH_3]_3$)
1c	7.83–6.22 (m, 24H, 4Ph and C_6H_4), 1.00 (s, 9H, *t*-C_4H_9NC)	268.1 (d, *J* 175, PPh_2), 201.9 (d, *J* 175, PPh_2)
1d	7.70–6.31 (m, 39H, 7Ph and C_6H_4)	273.1 (d, *J* 170, PPh_2), 189.0 (d, *J* 170, PPh_2), 42.5 (s, PPh_3)
1e	7.76–6.46 (m, 24H, 4Ph and C_6H_4), 2.46 (br, 3H, $P[CH(CH_3)_2]_3$), 1.27 (br, 9H, $P[CH(CH_3)_2]_3$)[d], 1.07 (br, 9H, $P[CH(CH_3)_2]_3$)[d]	267.1 (d, *J* 166, PPh_2), 175.0 (d, *J* 166, PPh_2), 55.6 (s, PPr^i_3)
2a	7.74–5.99 (m, 24H, 4Ph and C_6H_4)	170.8 (d, *J* 27, PPh_2), 150.0 (d, *J* 27, PPh_2)[c]
2b	7.81–6.27 (m, 24H, 4Ph and C_6H_4), 3.80 (d, J 12, 9H, $P[OCH_3]_3$), 3.45 (d. *J* 11, 9H, $P[OCH_3]_3$)	159.8 (ddd, J 269, 66, 27, PPh_2), 147.6 (ddd, *J* 66, 27, 2, $P[OCH_3]_3$), 141.1 (dd, *J* 269, 2, $P[OCH_3]_3$), 136.2 (dd, *J* 27, 2, PPh_2)
2c	7.76–6.10 (m, 24H, 4Ph and C_6H_4), 1.51 (s, 9H, *t*-C_4H_9NC), 1.29 (s, 9H, *t*-C_4H_9NC)	159.9 (d, *J* 31, PPh_2), 143.9 (d, *J* 31, PPh_2)
2d	7.76–6.01 (m, 39H, 7Ph and C_6H_4)[c]	169.4 (dd, J 40, 31, PPh_2), 132.2 (d, J 31, PPh_2), 41.5 (d, *J* 40, PPh_3)[c]
2e	8.04–6.32 (m, 24H, 4Ph and C_6H_4), 2.51 (d, J_{HH} 7, 3H, $P[CH(CH_3)_2]_3$)[e], 2.47 (d, J_{HH} 7, 3H, $P[CH(CH_3)_2]_3$)[e], 1.34 (dd, J_{PH} 15, J_{HH} 7, 9H, $P[CH(CH_3)_2]_3$)[d], 0.93 (dd, J_{PH} 14, J_{HH} 7, 9H, $P[CH(CH_3)_2]_3$)[d]	168.7 (dd, *J* 39, 29, PPh_2), 125.1 (d, *J* 29, PPh_2), 55.6 (d, *J* 39, PPr^i_3)

[a] CD_2Cl_2 solution unless otherwise stated.
[b] Coupling constant, *J*, in Hz.
[c] $CDCl_3$ solution.
[d] Diastereotopic methyls.
[e] Diastereotopic hydrogens.

The key question regarding the formation of **2a** is: does the benzoyl carbonyl arise from incoming CO or from a coordinated CO of **1a**? Intuitively the latter would be expected, i.e. that this is a migratory insertion reaction in which benzyne first migrates to coordinated CO, creating an unsaturated ruthenium centre to which external CO then coordinates. Labelling studies employing ^{13}C-enriched CO have shown that this is indeed the case. Thus, treatment of **1a** with ^{13}CO at room temperature gave complex **2a** with a ^{13}C-NMR spectrum which showed the label clearly confined to the terminal carbonyl sites, i.e. no enhancement of the benzoyl CO signal.

There is a variety of possible routes by which **1a** can be converted to **2a** through migratory insertion of CO and one plausible pathway is shown in Scheme 2. This envisages initial migration of benzyne to a coordinated CO to give **5**, containing a ligand of a type which is well established for alkyne-CO linking at a diruthenium centre [6]. This creates a 16-electron ruthenium centre, which accepts incoming CO to give **6**. Subsequent rearrangement of **6**, involving coordination of acyl oxygen and Ru–Ru bond cleavage, then produces the μ_3-benzoyl ligand in **7**, generating another 16-electron centre to which a second CO molecule can coordinate, giving **2a**. The appearance of labelled CO at all of the terminal carbonyl sites indicates that carbonyl scrambling must occur at some stage after the initial CO uptake has taken place.

The labelling study reveals that carbonylation is either irreversible or only very slowly reversible at r.t., since otherwise the label would enter the benzoyl CO group, but it is possible to regenerate **1a** quantitatively by warming complex **2a** in hexane or subjecting a toluene solution of **2a** to UV irradiation. This decarbonylation bears a striking resemblance to a previously reported reaction in which a benzyne complex $[Os_3(\mu\text{-}H)_2(CO)_9(\mu_3\text{-}C_6H_4)]$(**9**) is formed by heating the μ-benzoyl complex $[Os_3(\mu\text{-}H)(CO)_{10}(\mu\text{-}PhCO)]$ (**8**) [7]. In the light of our observations it is likely that the mechanism of this reaction involves CO loss followed by *ortho*-metallation to generate a complex containing a ligand similar to that in complex **2a**, which then undergoes decarbonylation to give benzyne.

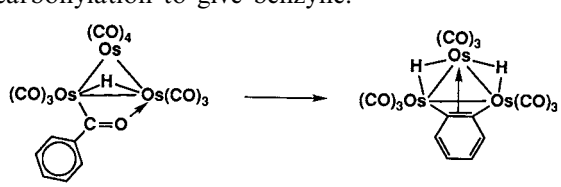

8 9

Table 3
^{13}C-NMR data for new complexes

Complex	^{13}C-NMR (δ)[a,b]
1b	c
1c	209.3 (d, *J* 9, CO), 203.6 (d, *J* 6, 2CO), 202.6 (t, *J* 9, CO), 199.5 (t, *J* 8, CO), 195.7 (s, CO), 162.4 (s, C_4H_9NC), 158.0 (d, *J* 16, Ru-bound C_6H_4), 153.3 (d, *J* 7, Ru-bound C_6H_4), 144.6 (d, *J* 21, *ipso*-C_6H_5), 143.0 (d, *J* 30, *ipso*-C_6H_5), 142.0-141.5 (m, 2*ipso*-C_6H_5), 134.3 (d, *J* 9), 132.6 (dd, *J* 16, 10), 131.9 (d, *J* 13), 130.5 (s), 130.0 (s), 129.3 (s), 128.3 (d, *J* 9), 128.0 (t, *J* 10), 127.4 (d, *J* 10) (Ph and C_6H_4), 29.8 (s, C_4H_9NC)
1d	208.4 (m, CO), 204.1 (m, CO), 200.4 (m, CO), 198.2 (m, CO), 197.5 (m, 2CO), 153.0 (br, Ru-bound C_6H_4), 157.2 (br, Ru-bound C_6H_4), 144.5 (d, *J* 24, *ipso*-C_6H_5), 144.1 (d, *J* 29, *ipso*-C_6H_5), 141.8 (d, *J* 24, *ipso*-C_6H_5), 141.1 (d, *J* 24, *ipso*-C_6H_5), 135.9 (d, *J* 42), 134.1 (d, *J* 11), 133.8 (d, *J* 9), 133.5 (d, *J* 9), 132.8 (d, *J* 9), 131.9 (d, *J* 11), 130.6 (s), 129.9 (s), 128.8 (s), 128.4 (s), 128.1 (t, *J* 11), 127.5 (t, *J* 8) (Ph and C_6H_4)
1e	209.3 (d, *J* 9, CO), 207.4 (t, *J* 10, CO), 206.8 (m, CO), 203.9 (dd, *J* 12, 5, CO), 201.9 (m, CO), 199.4-197.4 (m, CO), 158.3 (br, Ru-bound C_6H_4), 154.1 (br, Ru-bound C_6H_4), 144.6-144.2 (m, 3*ipso*-C_6H_5), 141.3 (d, *J* 26, *ipso*-C_6H_5), 134.5 (d, *J* 9), 133.9 (d, *J* 9), 132.9 (d, *J* 10), 132.1 (d, *J* 13), 130.6 (s), 130.0 (s), 129.0 (s), 128.0 (d, *J* 10), 127.5 (dd, *J* 31, 9), 32.0 (d, *J* 23, P[CH(CH_3)$_2$]$_3$)[d], 29.8 (d, *J* 23, P[CH(CH_3)$_2$]$_3$)[d], 20.2 (d, *J* 52, P[CH(CH_3)$_2$]$_3$)
2a	278.6 (dd, *J* 7, 4, C_6H_4CO), 198.9 (s, CO), 198.7 (d, *J* 11, CO), 198.2 (m, 2CO), 197.7 (s, CO), 197.1 (s, CO), 194.3 (d, *J* 9, CO), 193.3 (d, *J* 13, CO), 164.7 (d, *J* 12, substituted C_6H_4CO), 156.7 (d, *J* 13, substituted C_6H_4CO), 144.5 (d, *J* 32, *ipso*-C_6H_5), 139.6 (d, *J* 37, *ipso*-C_6H_5), 137.8 (d, *J* 26, *ipso*-C_6H_5), 136.3 (d, *J* 36, *ipso*-C_6H_5), 134.3 (d, *J* 11), 133.4 (d, *J* 10), 133.1 (d, *J* 11), 131.5 (s), 132.0 (s), 130.0 (s), 129.6 (s), 128.8 (d, *J* 11), 128.5 (d, *J* 10), 127.3 (s), 126.6 (d, *J* 10), 122.7 (s), 121.7 (s) (Ph and C_6H_4CO)
2b	282.0 (dd, *J* 4, 4, C_6H_4CO), 221.4 (ddd, *J* 21, 13, 8, CO), 204.3 (d, *J* 9, CO), 203.3-202.9 (m, 2CO), 202.6 (dd, *J* 14, 8, CO), 198.0 (dd, *J* 13, 8, CO), 169.2 (dd, *J* 19, 13, substituted C_6H_4CO), 158.8 (d, *J* 16, substituted C_6H_4CO), 146.6 (d, *J* 27, *ipso*-C_6H_5), 144.9 (d, *J* 3, *ipso*-C_6H_5), 140.8 (d, *J* 32, *ipso*-C_6H_5), 139.5 (d, *J* 7, *ipso*-C_6H_5), 139.1 (s), 134.7 (d, *J* 10), 134.0-133.5 (m), 129.3 (d, *J* 15), 128.5 (d, *J* 16), 128.0 (d, *J* 9), 127.7 (d, *J* 10), 126.4 (s), 126.3 (s), 121.4 (s), 120.4 (s) (Ph and C_6H_4CO), 52.7 (d, *J* 4, P[OCH_3]$_3$), 52.3 (d, *J* 6, P[OCH_3]$_3$)
2c	280.1 (m, C_6H_4CO), 220.5 (dd, *J* 20, 10, CO), 203.2 (d, *J* 10, 2CO), 201.0 (d, *J* 9, CO), 197.9 (d, *J* 8, CO), 196.2 (d, *J* 14, CO), 172.7 (d, *J* 12, substituted C_6H_4CO), 156.1 (d, *J* 12, substituted C_6H_4CO), 146.6 (d, *J* 26, *ipso*-C_6H_5), 144.1 (s),[e] 143.8 (s),[e] 141.4 (d, *J* 35, *ipso*-C_6H_5), 140.0 (d, *J* 21, *ipso*-C_6H_5), 138.5 (d, *J* 33, *ipso*-C_6H_5), 134.2 (d, *J* 10), 133.8 (d, *J* 9), 133.4 (dd, *J* 21, 10), 129.8 (s), 129.2 (s), 128.9 (s), 128.3 (d, *J* 9), 128.1-127.9 (m), 126.3 (s), 126.1 (d, *J* 9), 121.1 (s), 120.5 (s) (Ph and C_6H_4CO), 30.4 (s, C_4H_9NC), 30.3 (s, C_4H_9NC)
2d	279.8 (m, C_6H_4CO), 219.3 (d, *J* 15, CO), 205.4 (t, *J* 11, CO), 203.7 (d, *J* 7, CO), 203.0 (d, *J* 7, CO), 201.8 (d, *J* 7, CO), 200.7 (s, CO), 200.1 (s, CO), 199.1 (d, *J* 7, CO), 193.8 (d, *J* 9), 164.2 (d, *J* 12, substituted C_6H_4CO), 157.0 (d, *J* 12, substituted C_6H_4CO), 145.5 (d, *J* 32, *ipso*-C_6H_5), 144.8 (m, *ipso*-C_6H_5), 140.8 (d, *J* 29, *ipso*-C_6H_5), 138.4 (d, *J* 30, *ipso*-C_6H_5), 134.5 (m), 134.1 (dd, *J* 21, 11), 133.8-133.5 (m), 130.9 (s), 130.2 (s), 129.0 (s), 128.5 (s), 128.1 (d, *J* 10), 128.0 (s), 127.9 (s), 127.5 (t, *J* 10), 126.8 (d, *J* 10), 122.2 (d, *J* 22) (Ph and C_6H_4CO)[f]
2e	280.0 (m, C_6H_4CO), 220.0 (t, *J* 17, CO), 206.9 (t, *J* 11, CO), 205.7 (d, *J* 7, CO), 205.0 (d, *J* 7, CO), 202.0 (t, *J* 7, CO), 200.9 (s, CO), 200.3 (s, CO), 199.3 (d, *J* 7, CO), 192.9 (d, *J* 10, CO), 164.2 (d, *J* 10, substituted C_6H_4CO), 157.1 (d, *J* 10, substituted C_6H_4CO), 146.2-145.4 (m, 2*ipso*-C_6H_5), 142.4 (d, *J* 31, *ipso*-C_6H_5), 139.3 (d, *J* 22, *ipso*-C_6H_5), 134.6 (d, *J* 10), 134.2 (d, *J* 10), 134.0 (d, *J* 10), 133.8 (d, *J* 7), 133.3 (d, *J* 22), 131.2 (s), 129.2 (s), 128.6 (s), 128.3 (s), 128.2 (s), 127.5 (d, *J* 7), 127.2 (d, *J* 10), 126.7 (d, *J* 10), 122.7 (d, *J* 17) (Ph and C_6H_4CO), 28.4 (s, P[CH(CH_3)$_2$]$_3$),[d] 28.3 (s, P[CH(CH_3)$_2$]$_3$)[d], 20.0 (s, P[CH(CH_3)$_2$]$_3$)[d], 17.9 (s, P[CH(CH_3)$_2$]$_3$)[d]

[a] CD_2Cl_2 solution unless otherwise stated.
[b] Coupling constant *J* in Hz.
[c] Satisfactory data not obtained.
[d] Diastereotopic carbons.
[e] Due to impurity.
[f] $CDCl_3$ solution.

2.2. Reactions of $[Ru_3(CO)_7(\mu\text{-}PPh_2)_2(\mu_3\text{-}C_6H_4)]$ (**1a**) with PR_3 and ^{t}BuNC

Since the initial step in the reaction of **1a** with CO has been shown to be a migration of benzyne to coordinated CO followed by uptake of two molecules of externally provided CO, the reaction of **1a** with other π-acceptor ligands L could be expected to yield products $[Ru_3(CO)_6L_2(\mu\text{-}PPh_2)_2(\mu_3\text{-}C_6H_4CO)]$ similar to **2a**. This proved to be the case. Complex **1a** reacts with a 10–20-fold excess of $P(OMe)_3$ or ^{t}BuNC in dichloromethane at r.t. within 2 h to give complexes $[Ru_3(CO)_6L_2(\mu\text{-}PPh_2)_2(\mu_3\text{-}C_6H_4CO)]$(**2b**, **2c**) in 52 and 38% yields respectively. The use of only 2-fold excesses of the ligands gave, in addition to **2b** and **2c**, the mono-substituted complexes $[Ru_3(CO)_6(L)(\mu\text{-}PPh_2)_2(\mu_3\text{-}C_6H_4)]$(**1b**,**1c**), isolated in 25 and 16% yields, respectively. This suggests that, after migratory insertion and

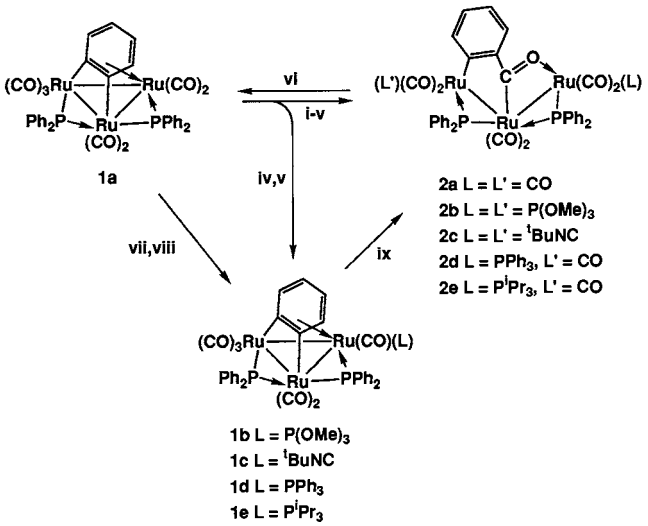

Scheme 1.

incorporation of one molecule of L, a decarbonylation pathway exists by which the *ortho*-metallated benzoyl ligand is reconverted to μ_3-benzyne.

The presence of two diphenylphosphido ligands in **1a** clearly causes crowding and, unlike $P(OMe)_3$ and ^{t}BuNC, the more bulky triphenylphosphine did not react with the complex at r.t. within 3 days. However, on heating **1a** with PPh_3 or P^iPr_3 in refluxing toluene for 2 h the complexes **1d** and **1e** were formed in 95 and 48% yields, respectively. When **1d** and **1e** are subjected to 2–3 atm of CO at r.t., the benzoyl complexes $[Ru_3(CO)_7(L)(\mu\text{-}PPh_2)_2(\mu_3\text{-}C_6H_4CO)]$ (**2d**,**2e**) are formed in ca. 50% yield within 5 days.

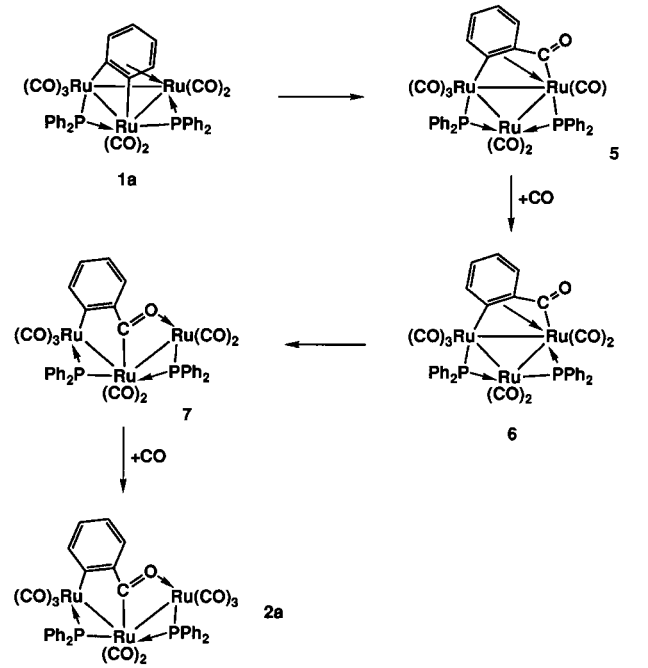

Scheme 2.

The complexes **1b**–**e** have spectroscopic data similar to those of the parent benzyne complex **1a** (Tables 1–3). It is clear from integration of the ^{1}H-NMR spectra that each complex contains a single molecule of PR_3 or ^{t}BuNC, confirmed by analytical data for all but **1c** which does, however, show a molecular ion in its mass spectrum. In view of the structure of **2e**, determined by X-ray diffraction (see below), the most likely site for the ligands L in the complexes **1b**–**e** is that shown in Scheme 1. However, the ^{31}P-NMR spectra of the PR_3 complexes **1b**, **1d** and **1e** differ in that while the first shows a doublet for the $P(OMe)_3$ phosphorus the last two show singlets for the corresponding PPh_3 and P^iPr_3 nuclei. This suggests that the $P(OMe)_3$ ligand is arranged *trans* to one of the μ-phosphido groups in **1b**, while in **1d** and **1e** the PPh_3 and P^iPr_3 ligands lie *cis*.

The spectroscopic data for complexes **2b-e** (Tables 1–3) are similar to those of **2a** and consistent with the structure depicted in Scheme 1. The presence of the benzoyl ligand in each is revealed by the characteristic carbonyl signal found at ca. δ 280 in the ^{13}C-NMR spectra, while ^{13}C- and ^{1}H-NMR data confirm the presence of two ligands L in **2b** and **2c**, and only one in **2d** and **2e**. A ^{1}H–^{1}H COSY experiment performed on complex **2b** has been used to fully characterise the complicated phenyl and *o*-metallated benzoyl ligand proton signals. The broad range of these signals range (δ 7.8–6.3 ppm) is attributed to ring current effects between neighbouring phenyl/benzoyl rings. The ^{31}P-NMR spectrum of **2b** is complicated, with coupling observed between all four phosphorus nuclei. The phosphido phosphorus nuclei in all complexes of type **2** show mutual coupling constants of ca. 30 Hz and thus the signals at δ 159.8 and 136.2 in **2b** are assigned to these ligands, while the remaining signals at δ 147.6 and 141.1 are assigned to the phosphite phosphorus nuclei. The ^{31}P{^{1}H}-NMR spectra of **2d** and **2e** both contain signals at ca. δ 170 and 130, consistent with two μ-phosphido ligands; the lower field signal also shows coupling to the phosphine phosphorus nucleus, which is found at ca. δ 50, and is thus attributed to the phosphido ligand which is bonded to the phosphine-substituted Ru atom.

Like **2a**, the complexes **2b** and **2c** are formed as fine yellow powders and also proved unsuitable for X-ray studies. Without such data it is difficult to determine how the two ligands L are distributed in the complexes, but the structure depicted in Scheme 1, which has the ligands bound to the 'terminal' ruthenium atoms of the cluster, appears clearly the most suitable on steric grounds; the central ruthenium, surrounded by the four phenyls of the phosphido groups, will be very crowded. If the pathway for ligand addition shown in Scheme 2 were followed it might have been expected that the two incoming PR_3 or ^{t}BuNC ligands would be bound to a single terminal ruthenium atom. However, the labelling

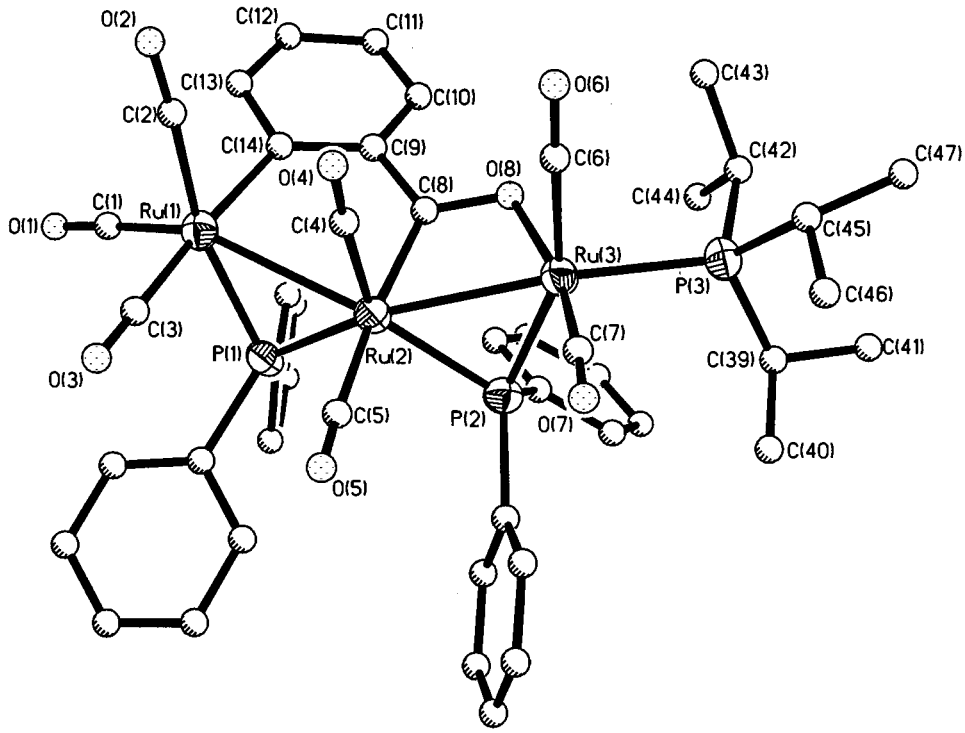

Fig. 1. Molecular structure of **2e** showing labelling scheme; all hydrogen atoms have been omitted for clarity.

study with ^{13}CO clearly showed CO scrambling over all the terminal carbonyl sites during the process and this will allow addition of PR_3 or ^{t}BuNC to occur so as to afford the thermodynamically most stable products.

Complex **2e** did give suitable crystals and an X-ray diffraction study was undertaken in order to establish the nature of the *ortho*-substituted benzoyl ligand.

2.3. Molecular structure of $[Ru_3(CO)_7(PPr^i_3)(\mu\text{-}PPh_2)_2(\mu_3\text{-}C_6H_4CO)]$ (**2e**)

The molecular structure of **2e** is shown in Fig. 1 and important bond lengths and angles are given in Table 4. The non-bonding Ru(1)–Ru(3) distance of 5.343(1) Å and Ru(1)–Ru(2)–Ru(3) bond angle of 143.1(1)° show that coordination of the benzoyl ligand is accompanied by opening of the Ru_3 triangle present in the precursor **1e**. The other Ru–Ru distances Ru(1)–Ru(2) and Ru(2)–Ru(3) of 2.849(1) and 2.783(1) Å are typical of Ru–Ru single bonds. The complex has a total of 50 cluster valence electrons in accord with this open triangle geometry. All of the carbonyl ligands in complex **2e** are terminal with the largest deviation from an ideal 180° Ru–C–O angle shown by the Ru(2)–C(5)–O(5) angle of 171.4(8)°. Both phosphido ligands bridge Ru–Ru bonds in symmetrical fashion. The bulky tri-isopropylphosphine ligand is bound to Ru(3) and is arranged effectively *cis* to the adjacent phosphido ligand [P(2)–Ru(3)–P(3) 107.5°], consistent with the small coupling observed between the phosphido and phosphine phosphorus nuclei in the ^{31}P-NMR spectrum.

The most interesting aspect of the molecular structure of **2e** is the coordination of the metallated benzoyl ligand, which bridges all three ruthenium atoms. Other published structures containing the benzoyl ligand bonded to metal clusters show coordination only of the acyl group to the metal atoms, and no *ortho*-metalation [8–10]. No clear pattern of bond length alternation is found in the *o*-metallated benzoyl ligand ring, although there may be some distortion, as indicated by the longest [C(13)–C(14) 1.441(12) Å] and shortest [C(11)–C(12) 1.364(14) Å] C–C bond distances. The carbonyl group bridges two ruthenium atoms in typical μ-acyl fashion with a C(8)–O(8) distance of 1.280(10) Å. This is about 0.06 Å longer than that found for typical aryl bound organic carbonyls [11] due to interaction between Ru(3) and O(8) removing electron density from the C(8)–O(8) bond. Evidence for a carbene component in the bonding between Ru(2) and the ligand is shown by a short Ru(2)–C(8) distance of 2.033(8) Å [cf. Ru(1)–C(14) 2.136(9) Å] and a tight Ru(3)–O(8)–C(8) bond angle of 103.5(5)° suggesting that O(8) may be sp^3 hybridised. Finally it is worth noting that Ru(2) is somewhat unusual in that it has approximately pentagonal bipyramidal coordination with C(8) and C(5) in the axial positions.

2.4. Hydrogenation of $[Ru_3(CO)_8(\mu\text{-}PPh_2)_2(\mu_3\text{-}C_6H_4CO)]$ (**2a**) and $[Ru_3(CO)_7(\mu\text{-}PPh_2)_2(\mu_3\text{-}C_6H_4)]$ (**1a**)

In an attempt to remove the new *ortho*-substituted

benzoyl ligand from complexation hydrogen was bubbled through a refluxing hexane solution of **2a** for 3 h. After this time the distinctive almond-like odour of benzaldehyde was clearly apparent and gas-liquid chromatography confirmed its presence, and also that of benzene, in a ratio of ca. 9:1. The IR spectrum of the reaction mixture indicated the fate of the triruthenium fragment, in showing the characteristic carbonyl bands of the known complex $[Ru_3(\mu\text{-}H)_2(CO)_8(\mu\text{-}PPh_2)_2]$(**10**) [12], which was isolated in 65% yield by column chromatography.

The likelihood that the minor benzene product arose from hydrogenation of complex **1a**, formed by decarbonylation of **2a**, was supported by heating a sample of the former in toluene, when **10** was formed quantitatively within 1 h, presumably with loss of benzene.

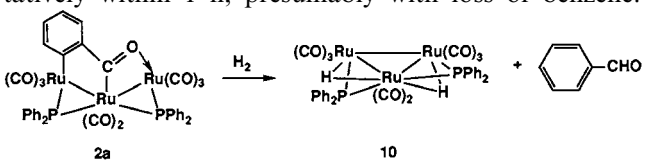

2a 10

Table 4
Selected bond lengths (Å) and angles (°) for complex **2e**

Ru(1)–Ru(2)	2.849(1)	Ru(1)···Ru(3)	5.343(1)
Ru(1)–C(1)	1.877(9)	Ru(1)–C(2)	1.962(10)
Ru(1)–C(3)	1.949(10)	Ru(1)–C(14)	2.136(9)
Ru(1)–P(1)	2.342(2)	Ru(2)–Ru(3)	2.783(1)
Ru(2)–C(4)	1.913(9)	Ru(2)–C(5)	1.957(10)
Ru(2)–C(8)	2.033(8)	Ru(2)–P(1)	2.367(2)
Ru(2)–P(2)	2.365(2)	Ru(3)–C(6)	1.942(10)
Ru(3)–C(7)	1.843(10)	Ru(3)–O(8)	2.170(6)
Ru(3)–P(2)	2.364(2)	Ru(3)–P(3)	2.388(3)
C(1)–O(1)	1.142(11)	C(2)–O(2)	1.122(13)
C(3)–O(3)	1.129(13)	C(4)–O(4)	1.142(12)
C(5)–O(5)	1.131(12)	C(6)–O(6)	1.119(12)
C(7)–O(7)	1.149(12)	C(8)–C(9)	1.492(12)
C(8)–O(8)	1.280(10)	C(9)–C(10)	1.387(13)
C(9)–C(14)	1.404(12)	C(10)–C(11)	1.384(13)
C(11)–C(12)	1.364(14)	C(12)–C(13)	1.385(14)
C(13)–C(14)	1.441(12)		
Ru(2)–Ru(1)–C(14)	85.1(2)	Ru(2)–Ru(1)–P(1)	53.2(1)
C(14)–Ru(1)–P(1)	91.7(2)	Ru(1)–Ru(2)–Ru(3)	143.1(1)
Ru(1)–Ru(2)–C(8)	84.6(2)	Ru(3)–Ru(2)–C(8)	68.0(2)
Ru(1)–Ru(2)–P(1)	52.4(1)	Ru(3)–Ru(2)–P(1)	150.9(1)
C(8)–Ru(2)–P(1)	96.9(2)	Ru(1)–Ru(2)–P(2)	150.8(1)
Ru(3)–Ru(2)–P(2)	53.9(1)	C(8)–Ru(2)–P(2)	85.5(2)
P(1)–Ru(2)–P(2)	101.9(1)	Ru(2)–Ru(3)–O(8)	69.4(2)
Ru(2)–Ru(3)–P(2)	54.0(1)	O(8)–Ru(3)–P(2)	82.1(2)
Ru(2)–Ru(3)–P(3)	156.7(1)	O(8)–Ru(3)–P(3)	96.2(2)
P(2)–Ru(3)–P(3)	107.5(1)	Ru(1)–C(1)–O(1)	177.3(8)
Ru(1)–C(2)–O(2)	175.3(9)	Ru(1)–C(3)–O(3)	176.4(9)
Ru(2)–C(4)–O(4)	174.1(8)	Ru(2)–C(5)–O(5)	171.4(8)
Ru(3)–C(6)–O(6)	178.6(7)	Ru(3)–C(7)–O(7)	174.9(8)
Ru(2)–C(8)–C(9)	126.7(6)	Ru(2)–C(8)–O(8)	117.7(6)
C(9)–C(8)–O(8)	115.5(7)	C(8)–C(9)–C(10)	118.9(8)
C(8)–C(9)–C(14)	118.5(8)	C(10)–C(9)–C(14)	122.6(8)
C(9)–C(10)–C(11)	12 0.8(8)	C(10)–C(11)–C(12)	
C(11)–C(12)–C(13)	122.0(9)	C(12)–C(13)–C(14)	121.1(8)
Ru(1)–C(14)–C(9)	123.9(6)	Ru(1)–C(14)–C(13)	121.3(6)
C(9)–C(14)–C(13)	114.8(8)	Ru(3)–O(8)–C(8)	103.5(5)
Ru(1)–P(1)–Ru(2)	74.5(1)	Ru(2)–P(2)–Ru(3)	72.1(1)

2.5. Conclusions

This work has described the reactions of the μ_3-benzyne complex **1a** with carbon monoxide and other π-acceptor ligands. The linking of CO with benzyne in the systems studied has been shown to be a low energy process, occurring at r.t. under 1 atm of CO. The process is readily reversed, with only gentle warming of the benzoyl product being required to regenerate the benzyne starting material. It has also been shown that the benzoyl ligand in complex **2a** may be removed by hydrogenation as benzaldehyde. This completes a pathway which may point to possible metal surface process for the conversion of benzene to benzaldehyde, namely: (i) adsorption of benzene, (ii) C–H activation to give benzyne plus surface hydrogen, (iii) benzyne linking with CO to yield a species analogous to that present in complexes **2**, and (iv) desorption of benzaldehyde following reaction with surface hydrogen. Step (i) has been well studied [1], (ii) has been modelled for a 111 surface in the transformation of $[Os_3(CO)_9(\mu_3\text{-}C_6H_6)]$ to $[Os_3H_2(CO)_9(\mu_3\text{-}C_6H_4)]$ [13] and for a step site on the same surface by the complex $[Ru_4(CO)_{11}(\mu\text{-}PPh)(\mu_5\text{-}C_6H_4)]$ [14], (iii) is modelled by **2a**, and (iv) by the reaction of **2a** with hydrogen.

3. Experimental

All reactions were carried out using dried and degassed solvents under a nitrogen atmosphere using standard Schlenk techniques. Photolysis reactions were carried out in silica glass tubes using a 500 W mercury vapour lamp as a UV irradiation source. Unless otherwise stated, separation of mixtures was carried out by pre-adsorbing the crude products onto alumina prior to chromatography on alumina columns (ca. 3×30 cm). IR spectra were recorded on a Perkin-Elmer 1710 Fourier Transform Spectrometer, using calcium fluoride cells of 1 mm path length. Proton, ^{13}C- and ^{31}P-NMR spectra were obtained using Jeol FX-90, GX-270 and GX-400 spectrometers. Elemental analyses were performed by the Microanalytical Laboratory of the School of Chemistry. Fast Atom Bombardment mass spectra were carried out by the EPSRC Mass Spectrometry Service Centre at the University of Swansea. GLC measurements were performed using a Perkin-Elmer 8600 GC instrument equipped with a BPI column. Carbon monoxide (BOC), hydrogen (BOC) and triphenylphosphine (Aldrich) were used as supplied. *t*-Butyl isocyanide, triisopropylphosphine and trimethylphosphite were distilled at reduced pressure prior to use. Complex **1a** was prepared by the method previously reported [2].

3.1. Carbonylation of $[Ru_3(CO)_7(\mu\text{-}PPh_2)_2(\mu_3\text{-}C_6H_4)]$ (1a)

(a) Carbon monoxide was bubbled through a solution of **1a** (100 mg, 0.106 mmol) in dichloromethane (150 cm^3) for 3 days, during which time the solution changed colour from dark red to yellow. The solvent was removed under reduced pressure to give **2a** in quantitative yield.

(b) A solution of complex **1a** (200 mg, 0.211 mmol) in toluene (50 cm^3) was subjected to carbon monoxide (3 atm) for 18 h in a Fischer-Porter vessel. The reaction mixture changed colour from dark red to yellow. The solvent was removed under reduced pressure and the residue was chromatographed on Florisil. Elution with hexane:dichloromethane (6:1) developed two bands. The first contained a trace of $[Ru_4(CO)_{11}(\mu_4\text{-}PPh)(\mu_4\text{-}C_6H_4)]$ [2] and the second gave 159 mg (75%) of $[Ru_3(CO)_8(\mu\text{-}PPh_2)_2(\mu_3\text{-}C_6H_4CO)]$ (**2a**) as a yellow powder after evaporaton of solvent.

3.2. Reaction of $[Ru_3(CO)_7(\mu\text{-}PPh_2)_2(\mu_3\text{-}C_6H_4)]$ (1a) with ^{13}C-enriched carbon monoxide

A diethyl ether (75 cm^3) solution of **1a** (150 mg, 0.159 mmol) was frozen by cooling to −196°C. The reaction vessel was placed under vacuum and then isolated from the vacuum pump before ^{13}C-enriched carbon monoxide (ca. 80 cm^3, 3.6 mmol) was introduced into the tube at atmospheric pressure. After 4 days stirring at r.t. the solution had changed colour from dark red to yellow. The solvent was removed under reduced pressure and the residue was chromatographed. Elution with hexane:dichloromethane (4:1) developed a single band containing the labelled product $[Ru_3(*CO)_8(\mu\text{-}PPh_2)_2(\mu_3\text{-}C_6H_4CO)]$ (**2a***).

3.3. Decarbonylation of $[Ru_3(CO)_8(\mu\text{-}PPh_2)_2(\mu_3\text{-}C_6H_4CO)]$ (2a)

(a) A solution of **2a** (26 mg, 0.026 mmol) in hexane (50 cm^3) slowly turned from yellow to red while being heated at reflux for 2 h. The solvent was removed under reduced pressure to give **1a** in quantitative yield.

(b) Nitrogen was slowly bubbled through a toluene (150 cm^3) solution of complex **2a** (50 mg, 0.053 mmol) while it was subjected to UV irradiation for 2.5 h. The solvent was removed under reduced pressure to leave a residue of **1a** in quantitative yield.

3.4. Reaction of $[Ru_3(CO)_7(\mu\text{-}PPh_2)_2(\mu_3\text{-}C_6H_4)]$ (1a) with trimethylphosphite

(a) Two equivalents of trimethylphosphite (0.04 cm^3, 0.317 mmol) and **1a** (150 mg, 0.159 mmol) in dichloromethane (50 cm^3) were stirred at r.t. for 24 h, then the solvent was removed under reduced pressure and the residue was chromatographed. Elution with hexane:dichloromethane (9:1) developed two yellow bands containing trace amounts of products that were not characterised. Further elution with hexane:dichloromethane (7:3) produced a red band containing 41 mg (25%) of $[Ru_3(CO)_6\{P(OMe)_3\}(\mu\text{-}PPh_2)_2(\mu_3\text{-}C_6H_4)]$(**1b**). Subsequent elution with hexane:dichloromethane (3:2) developed a yellow band from which 128 mg (67%) of $[Ru_3(CO)_6\{P(OMe)_3\}_2(\mu\text{-}PPh_2)_2(\mu_3\text{-}C_6H_4CO)]$ (**2b**) was obtained.

(b) To a dichloromethane (50 cm^3) solution of **1a** (100 mg, 0.105 mmol) 20 equiv. of trimethylphosphite (1.0 cm^3, 7.9 mmol) was added. After 2 h the solution had changed colour from red to yellow. The solvent was removed under reduced pressure and the residue was pre-adsorbed onto alumina and chromatographed. Elution with hexane:dichloromethane (3:2) developed a single yellow band containing 64 mg (52%) of complex **2b**.

3.5. Reaction of $[Ru_3(CO)_7(\mu\text{-}PPh_2)_2(\mu_3\text{-}C_6H_4)]$ (1a) with t-butyl isocyanide

(a) To a dichloromethane (50 cm^3) solution of **1a** (150 mg, 0.159 mmol) was added two equivalents of *t*-butyl isocyanide (0.036 cm^3, 0.317 mmol). After 24 h stirring at r.t. the solvent was removed under reduced pressure and the residue was chromatographed. Elution with hexane:dichloromethane (9:1) developed two yellow bands, which contained trace amounts of products that were not characterised, and a red band containing 26 mg (16%) of $[Ru_3(CO)_6(^tBuNC)(\mu\text{-}PPh_2)_2(\mu_3\text{-}C_6H_4)]$ (**1c**). Subsequent elution with hexane:dichloromethane (7:3) produced a red band containing 37 mg of a mixture of products that could not be separated. Further elution with hexane:dichloromethane (3:2) produced a yellow band containing 28 mg (16%) of $[Ru_3(CO)_6(^tBuNC)_2(\mu\text{-}PPh_2)_2(\mu_3\text{-}C_6H_4CO)]$ (**2c**).

(b) To a dichloromethane (60 cm^3) solution of **1a** (150 mg, 0.159 mmol) was added a 10-fold excess of *t*-butyl isocyanide (0.40 cm^3, 3.5 mmol). After 0.5 h the solution had changed colour from red to yellow. The solvent was removed under reduced pressure and the residue crystallised by slow diffusion of a pentane layer into a dichloromethane solution, which produced 60 mg (38%) of yellow microcrystalline **2c**.

3.6. Reaction of $[Ru_3(CO)_7(\mu\text{-}PPh_2)_2(\mu_3\text{-}C_6H_4)]$ (1a) with triphenylphosphine

A solution of **1a** (100 mg, 0.106 mmol) and

triphenylphosphine (100 mg, 0.381 mmol) in toluene (80 cm^3) was heated at reflux for 10 min. The solvent was removed under reduced pressure and the residue was chromatographed. Two bands were developed. The first, eluted with hexane:dichloromethane (9:1), gave a trace of unreacted complex **1a**. The second, eluted with hexane:dichloromethane (3:2) gave 118 mg (95%) of $[Ru_3(CO)_6(PPh_3)(\mu\text{-}PPh_2)_2(\mu_3\text{-}C_6H_4)]$ (**1d**).

3.7. Reaction of $[Ru_3(CO)_7(\mu\text{-}PPh_2)_2(\mu_3\text{-}\eta^2\text{-}C_6H_4)]$ (1a) with triisopropylphosphine

A solution of **1a** (278 mg, 0.294 mmol) and triisopropylphosphine (0.30 cm^3, 0.52 mmol) in toluene (50 cm^3) was heated at reflux for 1.5 h. The solvent was removed under reduced pressure and the residue was chromatographed. Elution with hexane:dichloromethane (19:1) developed three bands: first, unreacted complex **1a** (37 mg, 13%); second $[Ru_3(CO)_6(P^iPr_3)(\mu\text{-}PPh_2)_2(\mu_3\text{-}C_6H_4)]$ (**1e**) (152 mg, 48%) and third, 50 mg of a mixture of products that could not be separated.

3.8. Carbonylation of $[Ru_3(CO)_6(PPh_3)(\mu\text{-}PPh_2)_2(\mu_3\text{-}C_6H_4)]$ (1d)

A solution of **1d** (200 mg, 0.169 mmol) in toluene (50 cm^3) was subjected to CO (3 atm) for 5 days in a Fischer-Porter vessel. The reaction mixture changed colour from dark red to yellow. The solvent was removed under reduced pressure and the residue was chromatographed on Florisil. Elution with hexane:dichloromethane (4:1) developed two bands. The first contained a trace of unreacted **1d** and the second gave 105 mg (50%) of $[Ru_3(CO)_7(PPh_3)(\mu\text{-}PPh_2)_2(\mu_3\text{-}C_6H_4CO)]$ (**2d**).

3.9. Carbonylation of $[Ru_3(CO)_6(P^iPr_3)(\mu\text{-}PPh_2)_2(\mu_3\text{-}\eta^2\text{-}C_6H_4)]$ (1e)

A solution of **1e** (260 mg, 0.241 mmol) in diethyl ether (50 cm^3) was subjected to carbon monoxide (2 atm) for 17 h in a Fischer-Porter vessel, during which time the reaction mixture changed colour from dark red to yellow. The solvent was removed under reduced pressure and the residue was chromatographed. Elution with hexane:dichloromethane (19:1) gave 10 mg (4%) of complex **1a**. Further elution with hexane:dichloromethane (9:1) produced three bands. The first gave 15 mg (6%) of **2a**, the second 35 mg of unreacted complex **1e**, and the third 120 mg (44%) of $[Ru_3(CO)_7(P^iPr_3)(\mu\text{-}PPh_2)_2(\mu_3\text{-}C_6H_4CO)]$ (**2e**).

3.10. Hydrogenation of $[Ru_3(CO)_8(\mu\text{-}PPh_2)_2(\mu_3\text{-}C_6H_4CO)]$ (2a)

Hydrogen was bubbled through a refuxing hexane (150 cm^3) solution of **2a** (27 mg, 0.027 mmol) for 3 h. A sample of the reaction mixture was then analysed by GLC, revealing the presence of benzaldehyde and benzene in 9:1 ratio. After removal of solvet under reduced pressure the residue was chromatographed on Florisil. Elution with hexane:dichloromethane (9:1) developed two bands. The first gave 15 mg (65%) of yellow $[Ru_3(\mu\text{-}H)_2(CO)_8(\mu\text{-}PPh_2)_2]$(**10**) [12], identified by IR and-NMR spectroscopy. The second contained a trace of complex **1a**.

3.11. Hydrogenation of $[Ru_3(CO)_7(\mu\text{-}PPh_2)_2(\mu_3\text{-}C_6H_4)]$ (1a)

Hydrogen was bubbled through a solution of **1a** (50 mg, 0.053 mmol) in toluene (150 cm^3) while heating at reflux for 1 h. The solvent was removed under reduced pressure to give yellow $[Ru_3(\mu\text{-}H)_2(CO)_8(\mu\text{-}PPh_2)_2]$ (**10**) in quantitative yield.

3.12. Structure determination for $[Ru_3(CO)_7(P^iPr_3)(\mu\text{-}PPh_2)_2(\mu_3\text{-}C_6H_4CO)]$ (2e)

Crystal data: $C_{47}H_{45}O_8P_3Ru_3$, $M = 1134.0$, orthorhombic, space group *Pbca* (no. 61), $a = 19.448(6)$, $b = 19.568(6)$, $c = 24.135(8)$ Å, $U = 9180(6)$ $Å^3$, $Z = 8$, $D_{calc} = 1.64$ g cm^{-3}, $\Delta = 0.7107$ Å, $\mu(Mo\text{–}K_\alpha) = 11.1$ cm^{-1}, $F(000) = 4432$, $T = 293$ K.

A single crystal of **2e** (approximate dimensions $0.3 \times 0.2 \times 0.1$ mm) was mounted in a thin-walled glass capillary and held in place with epoxy glue. All diffraction measurements were made at r.t. (293 K) on a Siemens four-circle R3m/V diffractometer, using graphite monochromated $Mo\text{–}K_\alpha$ X-radiation. Unit cell dimensions were determined from 29 centred reflections in the range $15 < 2\theta < 26°$. A total of 9457 diffracted intensities, including check reflections, were measured in a unique octant of reciprocal space for $4 < 2\theta < 50°$ by Wyckoff ω scans. Three check reflections ($-7\ 0\ 4$, $-1\ -7\ 4$, $-3\ -5\ 7$) remeasured after every 50 ordinary data showed no significant decay over the period of data collection. Of all the intensity data collected, 8131 unique observations remained after averaging of duplicate and equivalent measurements and deletion of systematic absences, of these 4700 with $I > 2\sigma(I)$ were retained for use in structure solution and refinement. An absorption correction was applied on the basis of 432 azimuthal scan data, maximum and minimum transmission coefficients being 0.291 and 0.261, respectively. Lorentz and polarisation corrections were applied.

The structure was solved by Patterson and Fourier methods. All non-hydrogen atoms were assigned anisotropic displacement parameters and all hydrogen atoms fixed isotropic displacement parameters. All non-hydrogen atoms were refined without positional con-

Table 5
Atomic co-ordinates ($\times 10^4$) for complex **2e**

Atom	*x*	*y*	*z*
Ru(1)	4971(1)	2185(1)	2663(1)
Ru(2)	4585(1)	2082(1)	1527(1)
Ru(3)	3990(1)	1210(1)	752(1)
C(1)	4945(5)	2718(5)	3309(4)
C(2)	5276(5)	1310(5)	2974(4)
C(3)	5895(5)	2441(5)	2427(4)
C(4)	5064(5)	1270(5)	1743(4)
C(5)	5428(5)	2361(5)	1146(4)
C(6)	4246(5)	305(5)	1011(4)
C(7)	4684(5)	1178(4)	233(4)
C(8)	3725(4)	1621(4)	1827(4)
C(9)	3499(5)	1595(4)	2418(3)
C(10)	2840(5)	1369(4)	2538(4)
C(11)	2608(5)	1339(5)	3079(4)
C(12)	3045(5)	1529(5)	3494(4)
C(13)	3708(5)	1750(4)	3388(3)
C(14)	3961(4)	1810(4)	2829(3)
C(15)	5162(4)	3742(4)	1967(4)
C(16)	5449(5)	4110(4)	2404(4)
C(17)	5865(6)	4673(5)	2315(6)
C(18)	6000(6)	4865(5)	1778(6)
C(19)	5730(6)	4516(5)	1334(5)
C(20)	5310(5)	3947(4)	1427(4)
C(21)	3809(4)	3594(4)	2319(4)
C(22)	3289(5)	3353(5)	2663(4)
C(23)	2753(5)	3776(5)	2822(4)
C(24)	2738(6)	4446(5)	2657(5)
C(25)	3241(6)	4679(6)	2326(5)
C(26)	3779(5)	4270(5)	2150(5)
C(27)	3019(4)	2749(4)	852(4)
C(28)	2631(5)	2908(4)	382(4)
C(29)	1947(6)	3120(5)	425(5)
C(30)	1654(6)	3184(6)	931(5)
C(31)	2026(5)	3061(5)	1403(5)
C(32)	2708(5)	2836(5)	1371(4)
C(33)	4250(4)	3034(4)	287(3)
C(34)	4050(6)	3726(5)	313(4)
C(35)	4367(6)	4209(5)	−12(5)
C(36)	4881(6)	4017(6)	−383(4)
C(37)	5086(6)	3347(5)	−411(4)
C(38)	4775(5)	2860(5)	−86(4)
C(39)	2768(5)	1408(5)	−340(4)
C(40)	3310(6)	1731(5)	−707(4)
C(41)	2141(6)	1188(6)	−681(5)
C(42)	2346(5)	505(5)	538(4)
C(43)	2496(7)	−46(6)	963(4)
C(44)	1953(5)	1096(6)	801(5)
C(45)	3356(6)	−13(5)	−234(4)
C(46)	3905(7)	98(7)	−663(5)
C(47)	2783(6)	−437(6)	−472(5)
O(1)	4930(4)	3065(4)	3689(3)
O(2)	5457(4)	832(4)	3186(3)
O(3)	6435(4)	2555(4)	2284(3)
O(4)	5353(4)	773(3)	1824(3)
O(5)	5922(3)	2438(4)	907(3)
O(6)	4384(4)	−222(4)	1152(3)
O(7)	5151(4)	1156(4)	−59(3)
O(8)	3350(3)	1288(3)	1485(2)
P(1)	4539(1)	3062(1)	2101(1)
P(2)	3884(1)	2413(1)	772(1)
P(3)	3112(1)	781(1)	154(1)

traints. All hydrogen atoms were constrained to idealised geometries (C–H 0.96 Å) with fixed isotropic displacement parameters. Full-matrix least squares refinement of this model (550 parameters) converged to final residual indicies $R = 0.048$, $R' = 0.043$, $S = 1.16$, where $R = \Sigma|\Delta|/\Sigma|F_o|$; $R' = (\Sigma w\Delta^2/\Sigma wF_o^2)^{0.5}$; $S = [\Sigma w\Delta^2/(N_o - N_v)]^{0.5}$; $\Delta = F_o - F_c$ and N_o, N_v = number of observations and of variables. Weights, w, were set equal to $[\sigma_c^2(F_o) + gF_o^2]^{-1}$, where $\sigma_c^2(F_o)$ is the variance in F_o due to counting statistics and $g = 0.0004$ was chosen to minimise the variation if S as a function of $|F_o|$. Final electron-density difference maps showed no features outside the range $+0.3$ to -0.3 eÅ^{-3}, the largest of these being close to the ruthenium atoms. Table 5 lists the final atomic positional parameters for the freely refined atoms, and Table 4 the selected bond lengths and inter-bond angles. All calculations were carried out using programs of the SHELXTL package [15]. Complex neutral-atom scattering factors were taken from ref. [16].

Additional information available from the Cambridge Crystallographic Data Centre comprises H-atom co-ordinates, thermal parameters and remaining bond lengths and angles.

Acknowledgements

We are grateful to the EPSRC for the award of Research Studentships (to JPHC, HAAD, and NJG) and for support, the EU through the framework of the Community Science programme for support, and CIRIT (Generalitat de Catalunya) for travel grants (to JMV).

References

[1] E.L. Muetterties, Pure Appl. Chem. 54 (1982) 83.
[2] S.A.R. Knox, B.R. Lloyd, D.A.V. Morton, S.M. Nicholls, A.G. Orpen, J.M. Viñas, M. Weber, G.K. Williams, J. Organomet. Chem. 394 (1990) 385.
[3] E.L. Muetterties, T.N. Rhodin, E. Band, C.F. Brucker, W.W. Pretzer, Chem. Rev. 79 (1979) 91.
[4] M.J. Burn, G.-Y. Kiel, F. Seils, J. Takats, J. Washington, J. Am. Chem. Soc. 111 (1989) 6850.
[5] J.P.H. Charmant, H.A.A. Dickson, N.J. Grist, J.B. Keister, S.A.R. Knox, D.A.V. Morton, A.G. Orpen, J.M. Viñas, J. Chem. Soc. Chem. Commun. (1991) 1393.
[6] A.F. Dyke, S.A.R. Knox, P.J. Naish, G.E. Taylor, J. Chem. Soc. Dalton Trans. (1982) 1297.
[7] K.A. Azam, C.C. Yin, A.J. Deeming, J. Chem. Soc. Dalton Trans. (1978) 1201.
[8] N. Lugan, G. Lavigne, J.J. Bonnet, Inorg. Chem. 25 (1986) 7.
[9] J.R. Blickensderfer, C.B. Knobler, H.D. Kaesz, J. Am. Chem. Soc. 97 (1975) 2681.
[10] J.R. Blickensderfer, C.B. Knobler, H.D. Kaesz, J. Am. Chem. Soc. 97 (1975) 2686.

[11] A.G. Orpen, L. Brammer, F.H. Allen, O. Kennard, D.G. Watson, R. Taylor, J. Chem. Soc. Dalton Trans. (1989) S1.
[12] V.D. Patel, A.A. Cherkas, D. Nucciarone, N.J. Taylor, A.J. Carty, Organometallics 4 (1985) 1792.
13] M.A. Gallop, B.F.G. Johnson, J. Lewis, A. McCamley, R.N. Perutz, J. Chem. Soc. Chem. Commun. (1988) 1071.
[14] S.A.R. Knox, B.R. Lloyd, A.G. Orpen, J.M. Viñas, M. Weber, J. Chem. Soc. Chem. Commun. (1987) 1498.
[15] G.M. Sheldrick, SHELXTL, Revision 5.1, Göttingen, 1986.
[16] International Tables for X-ray Crystallography, vol. 4, Kynoch Press, Birmingham, 1974.